

## Supporting Information

for

### **Creation of glycoprotein imprinted self-assembled monolayers with dynamic boronate recognition sites and imprinted cavities for selective glycoprotein recognition**

Xianfeng Zhang<sup>a,b</sup> and Xuezhong Du<sup>a,\*</sup>

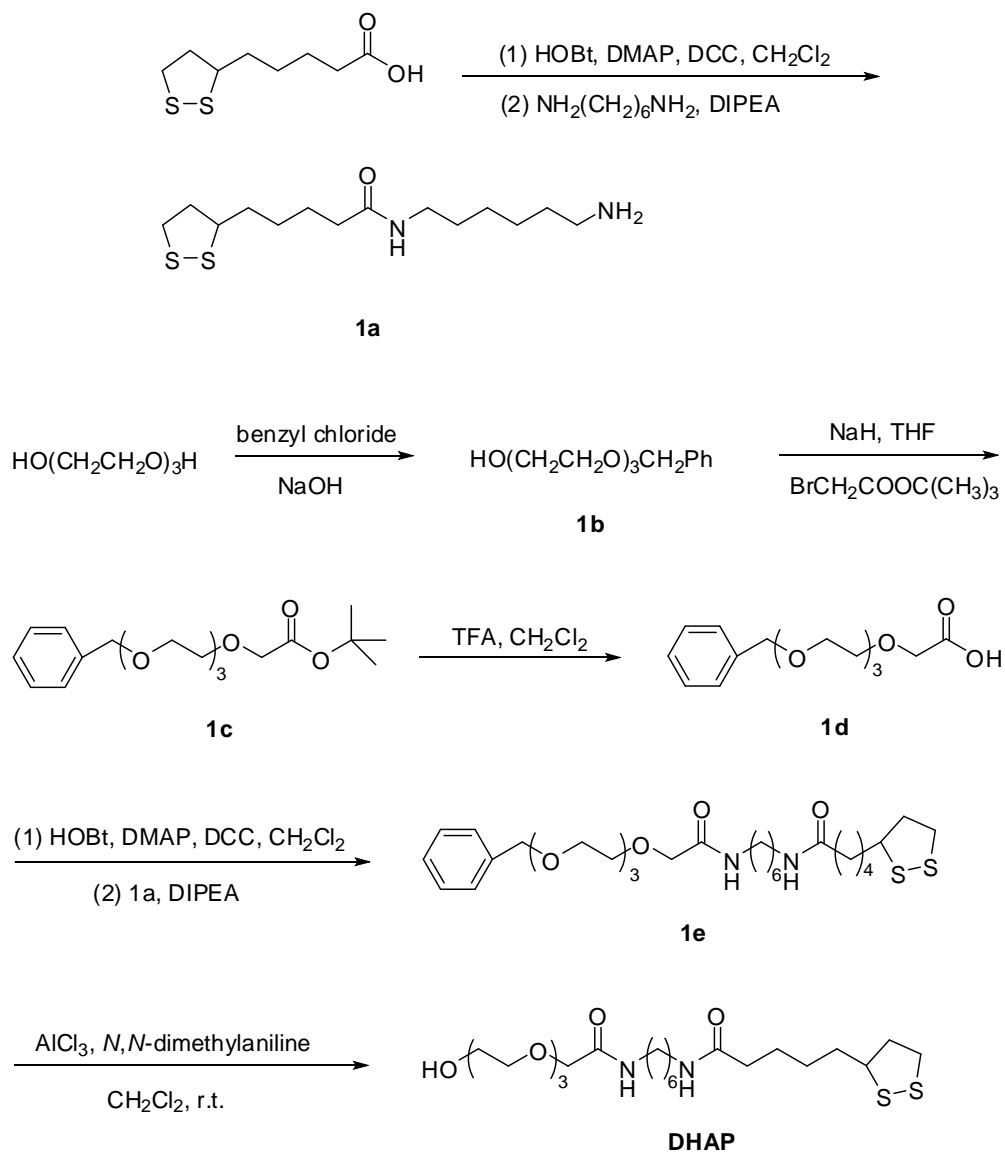
<sup>a</sup> *Key Laboratory of Mesoscopic Chemistry (Ministry of Education), State Key Laboratory of Coordination Chemistry, Collaborative Innovation Center of Chemistry for Life Sciences, and School of Chemistry and Chemical Engineering, Nanjing University, Nanjing 210023, People's Republic of China*

<sup>b</sup> *School of Material and Chemical Engineering, Bengbu University, Bengbu 233030, People's Republic of China*

E-mail: xzdu@nju.edu.cn

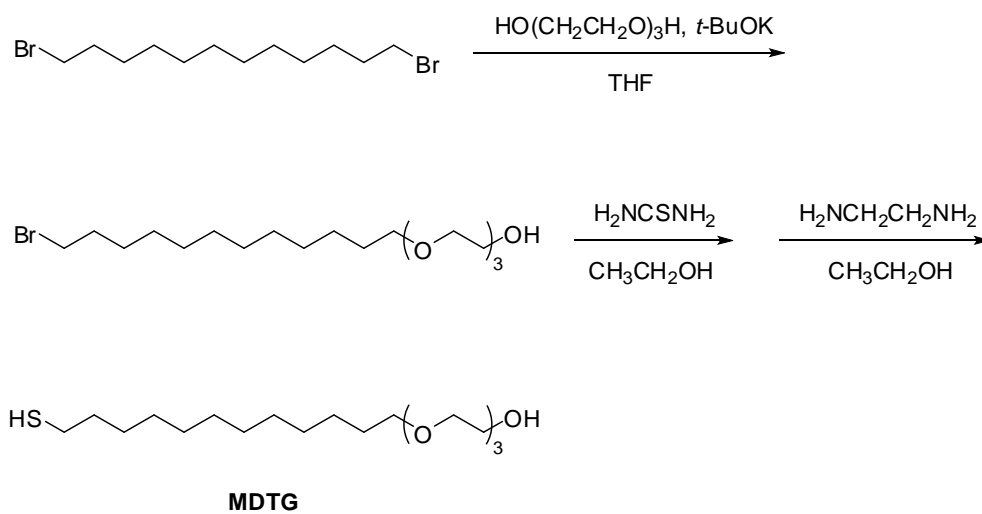
## Synthesis of DHAP

DHAP was synthesized according to our previous work.<sup>S1</sup> The synthetic route to DHAP was described in the following:



## Synthesis of MDTG

MDTG was synthesized according to our previous work.<sup>S1</sup> The synthetic route to MDTG was described in the following:



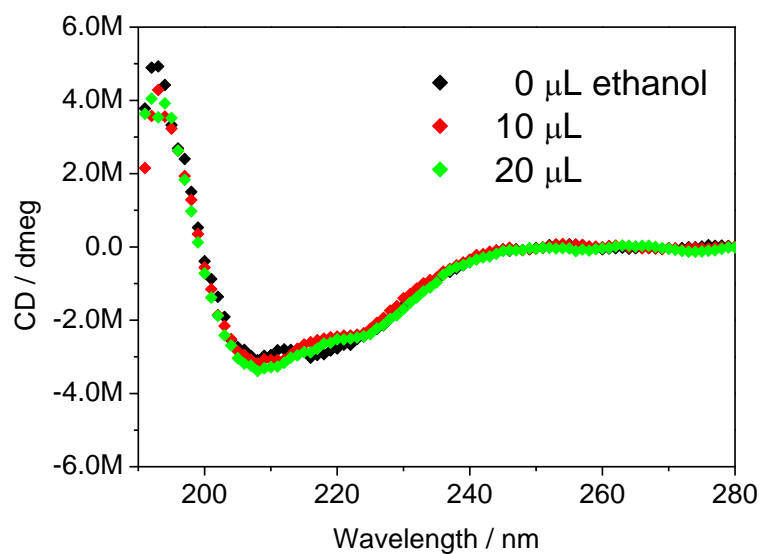


**Fig. S1** CD spectra of HRP (46  $\mu\text{g}/\text{mL}$ ) in 0.5 mL PBS solution (pH = 7.4) upon addition of ethanol with different amounts.

In the UV region of CD spectra, the primary chromophores of proteins are peptides related to the information on conformations of proteins. Two negative peaks at 222 and 208 nm and one positive peak around 190 nm are indicative of  $\alpha$ -helix conformation. The CD spectra of HRP in the PBS solution remained almost unchanged in the presence of 10–20  $\mu\text{L}$  ethanol, which indicates that the conformations of HRP were unaffected upon addition of a very small amount of ethanol.

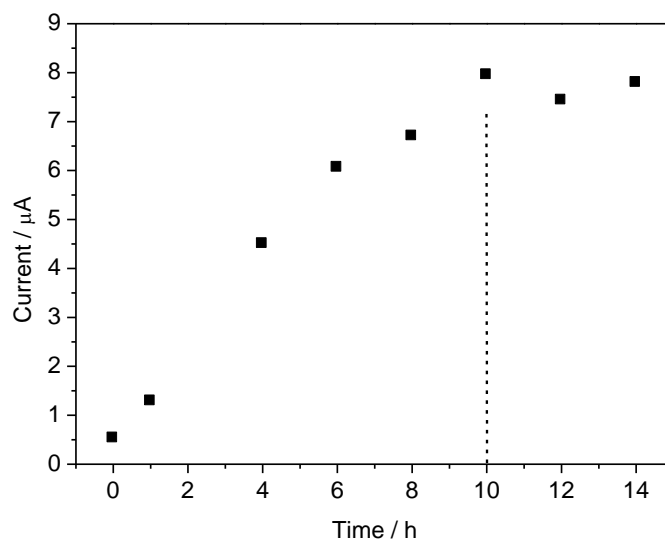


**Fig. S2** DPV cathodic peak current of HRP-imprinted SAM coated electrode from DHAP and PMBA/PATP as a function of elution time with aqueous solution of acetic acid (10 mM, pH = 3.1) and subsequently with double-distilled water. The DPV curves of the HRP-imprinted electrodes were measured in 10 mM PBS solution (pH = 7.4) of 2.5 mM  $\text{Fe}(\text{CN})_6^{4-/3-}$  and 0.1 M KCl.

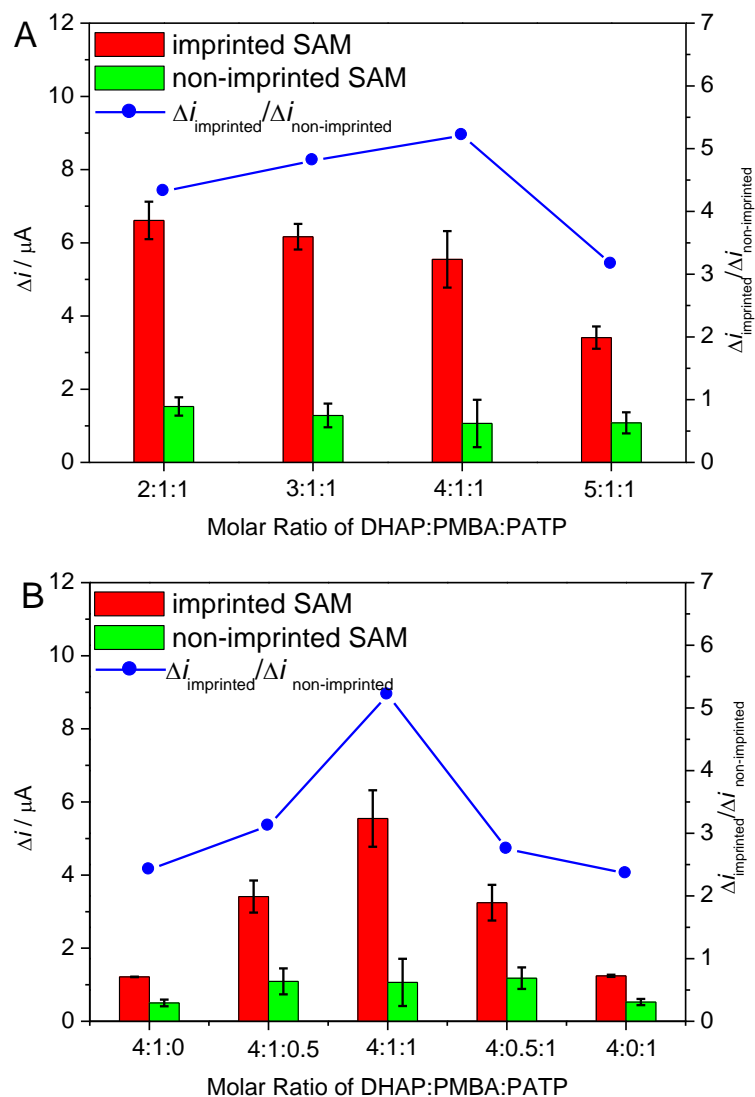


**Fig. S3** Change in DPV cathodic peak current ( $\Delta i$ ) after and before HRP binding and the ratio of peak current change of the HRP-imprinted SAM coated electrodes to non-imprinted one against the molar ratio of DHAP:PMBA:PATP: (A) the molar ratio of PMBA:PATP was fixed at 1:1; (B) the amount of DHAP was fixed. The DPV curves of the HRP-imprinted and non-imprinted electrodes were measured in 10 mM PBS solution (pH = 7.4) of 2.5 mM  $\text{Fe}(\text{CN})_6^{4-/3-}$  and 0.1 M KCl.

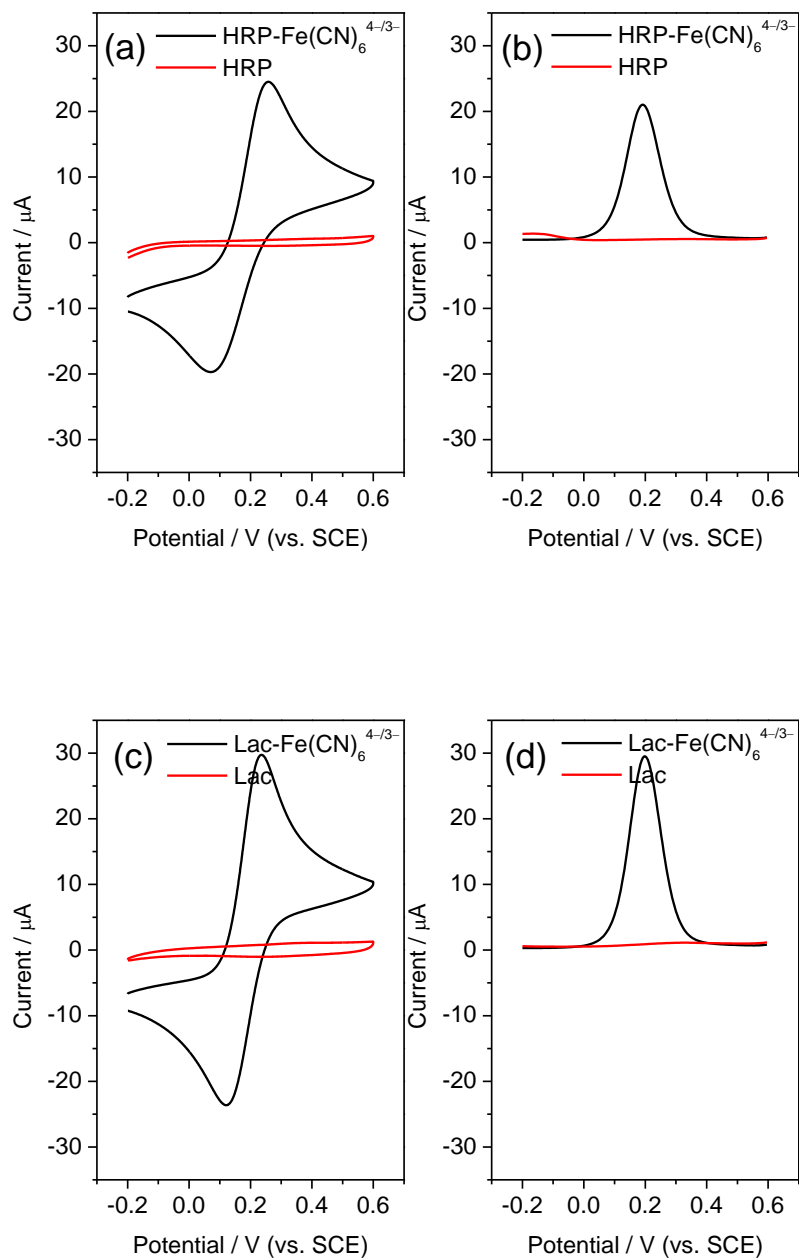


**Fig. S4** CV and DPV curves of bare gold electrodes toward different proteins at 120  $\mu\text{g/mL}$  in 10 mM PBS solution (pH = 7.4) in the absence and presence of  $\text{Fe}(\text{CN})_6^{4-/3-}$ : (a,b) HRP; (c,d) Lac; (e,f) Mb; (g,h) BHb.

The proteins themselves showed no or almost no redox peak. The decrease in peak current in the presence of  $\text{Fe}(\text{CN})_6^{4-/3-}$  was owing to the adsorption of protein onto the gold electrode. The order of protein adsorption was BHb > Mb > HRP > Lac.

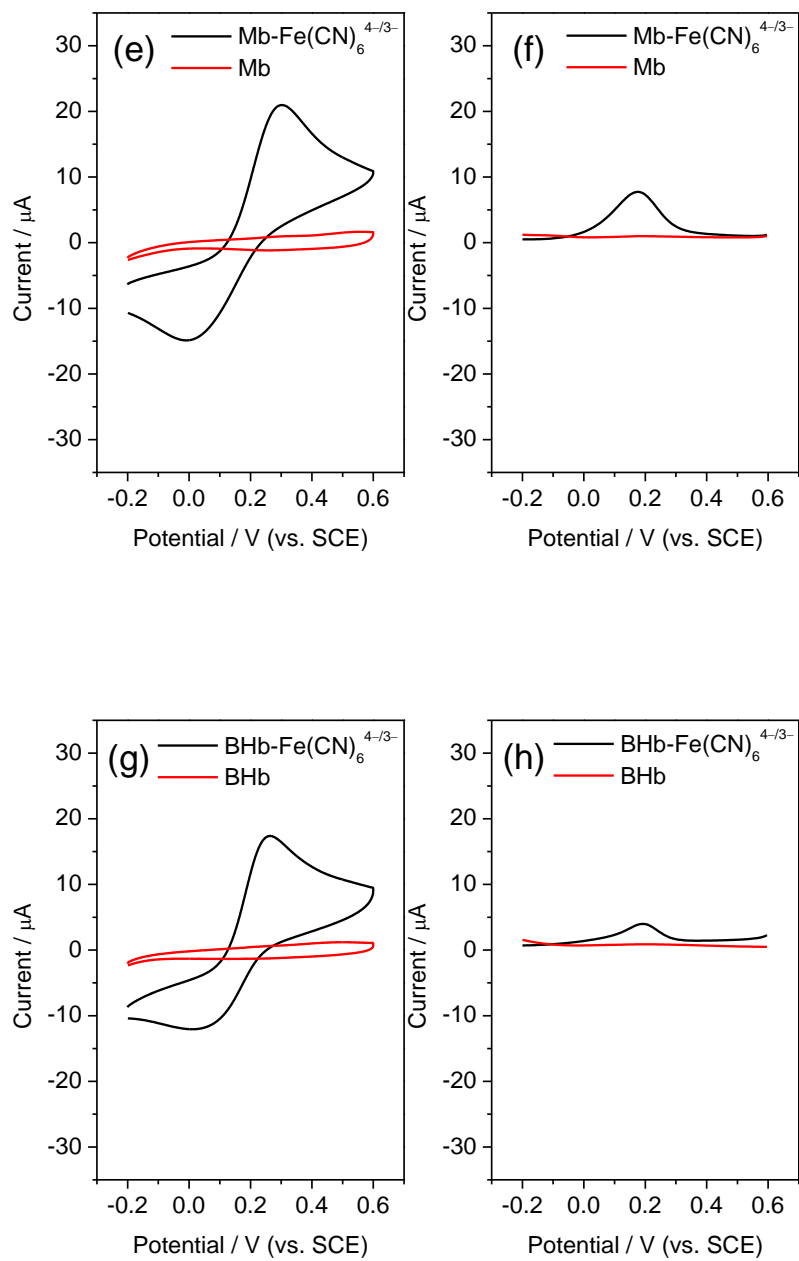


**Fig. S4** (continued)



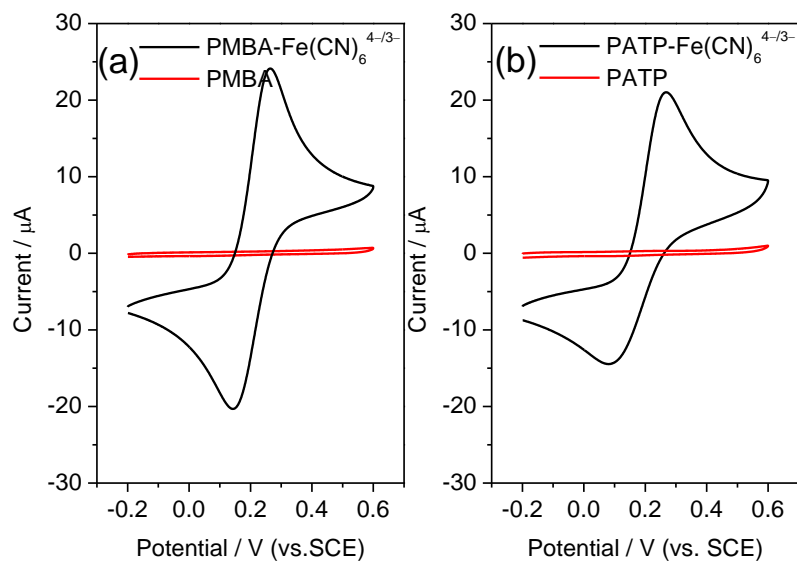


**Fig. S5** CV curves of (a) PMBA- and (b) PATP-modified gold electrodes in 10 mM PBS solution (pH = 7.4) in the absence and presence of  $\text{Fe}(\text{CN})_6^{4-/3-}$ .

The PMBA- and PATP-modified SAM coated electrodes themselves showed no redox peak from respective CV curves, which indicates that PMBA and PATP themselves could not affect the electrochemical measurements.

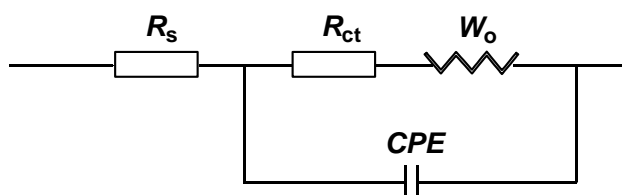


**Fig. S6** Modified Randles' equivalent circuit model was used to fit the EIS curves in Fig. 1:  $R_s$ , solution resistance;  $R_{ct}$ , charge transfer resistance;  $W_o$ , finite diffusion impedance;  $CPE$ , constant phase angle element associated with double layer capacitance.

**Table S1** Electrochemical parameters extracted from the EIS curves of various electrodes in Fig. 1.

electrode	$R_s$ ( $\Omega$ )	$R_{ct}$ ( $\Omega$ )	$W_o$ -R ( $\Omega$ )	$W_o$ -T ( $\Omega$ )	$W_o$ -P ( $\Omega$ )	$CPE$ -T ( $10^{-6}$ ) ( $\Omega^{-1}\cdot\text{cm}^{-2}\cdot\text{s}^P$ )	$CPE$ -P
a	140	623	25766	857	0.4642	8.9665	0.7276
b	192	66334	35487	806	0.3203	0.6317	0.8721
c	188	11580	20191	490	0.4919	1.0606	0.8476
d	203	22074	30467	887	0.3669	1.9423	0.8521
e	178	69420	21892	574	0.2599	3.2755	0.8315

a: bare gold electrode

b: imprinted electrode from DHAP and PMBA/PATP before HRP extraction

c: imprinted electrode from DHAP and PMBA/PATP after HRP extraction

d: imprinted electrode from DHAP and PMBA/PATP upon addition of HRP (18  $\mu\text{g/mL}$ )

e: non-imprinted electrode

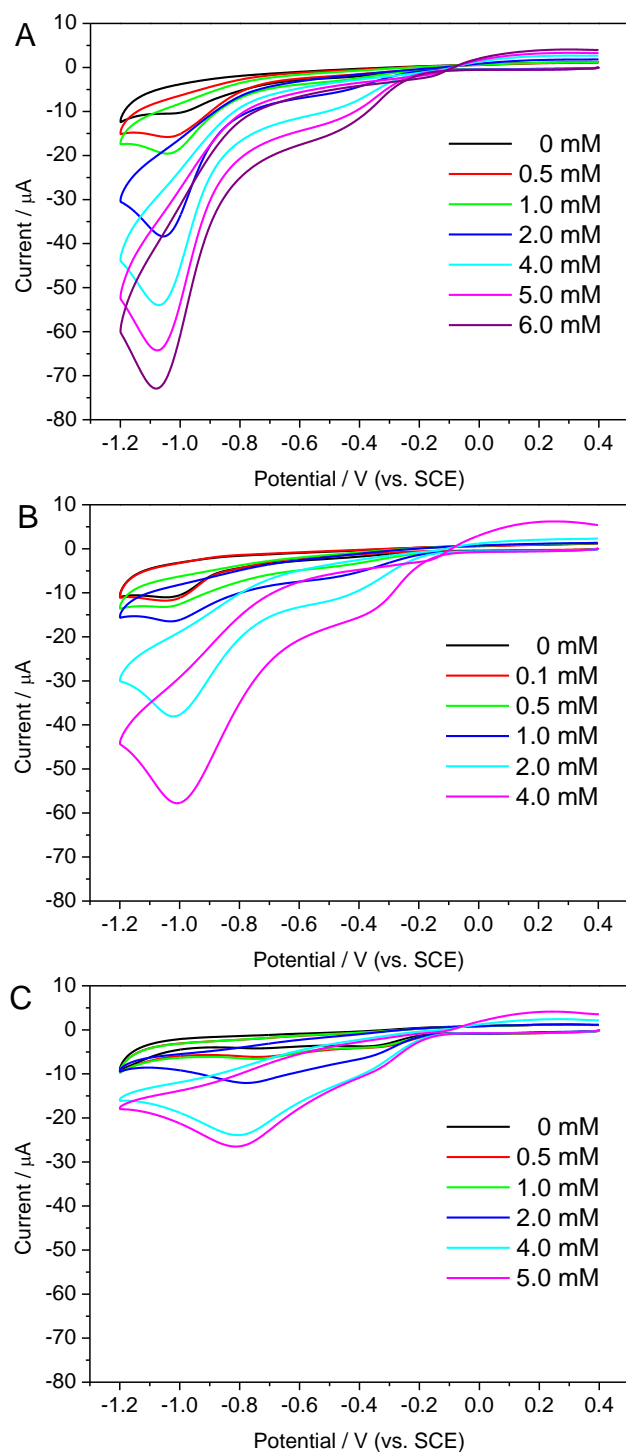


**Fig. S7** CV curves of various kinds of HRP-bound gold electrodes toward  $\text{H}_2\text{O}_2$  of different concentrations at 100 mV/s in  $\text{N}_2$ -saturated PBS solution (pH = 7.4): (A) HRP-imprinted SAM coated gold electrode from DHAP and PMBA/PATP; (B) HRP-bound SAM coated gold electrode from PMBA/PATP; (c) HRP-adsorbed gold electrode.

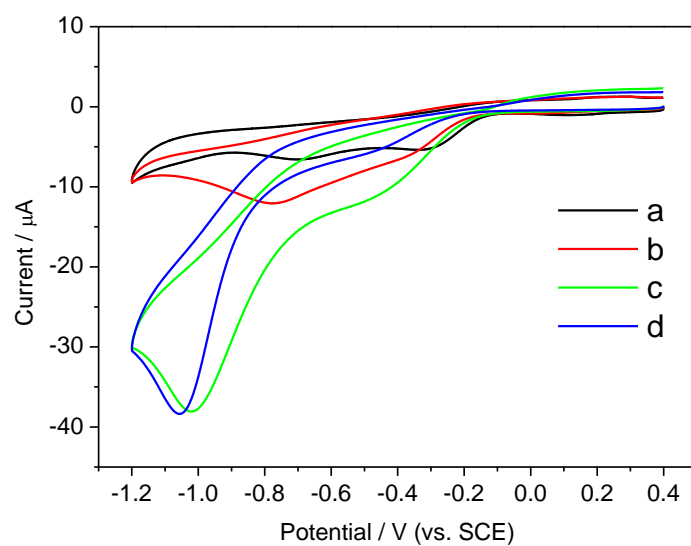


**Fig. S8** CV curves of various kinds of electrodes toward 2 mM  $\text{H}_2\text{O}_2$  at 100 mV/s in  $\text{N}_2$ -saturated PBS solution (pH = 7.4): (a) bare gold electrode; (b) HRP-adsorbed gold electrode; (c) HRP-bound SAM coated gold electrode from PMBA/PATP; (d) HRP-imprinted SAM coated gold electrode from DHAP and PMBA/PATP.

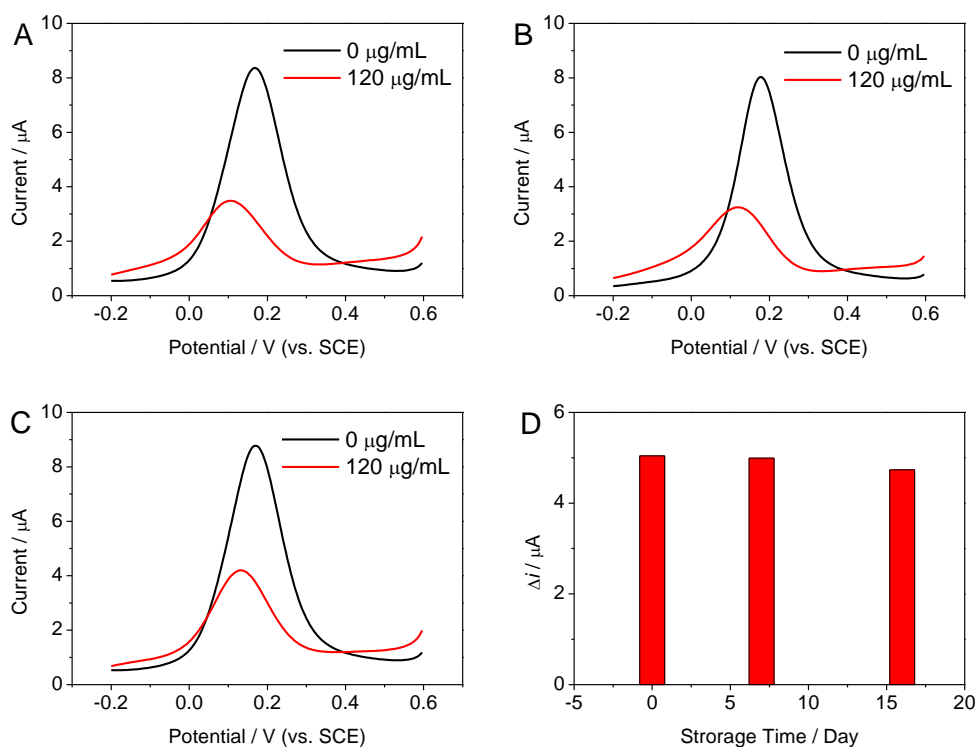


**Fig. S9** DPV cathodic peak currents of the HRP-imprinted SAM coated electrode from DHAP and PMBA/PATP before and after addition of 120  $\mu\text{g/mL}$  HRP in 10 mM PBS solution (pH = 7.4) of 2.5 mM  $\text{Fe}(\text{CN})_6^{4-/3-}$  and 0.1 M KCl: (A) freshly prepared; (B) stored for 7 days; (C) stored for 16 days. (D) Decrease of DPV cathodic peak currents of the HRP-imprinted electrode upon addition of 120  $\mu\text{g/mL}$  HRP for different storage times.

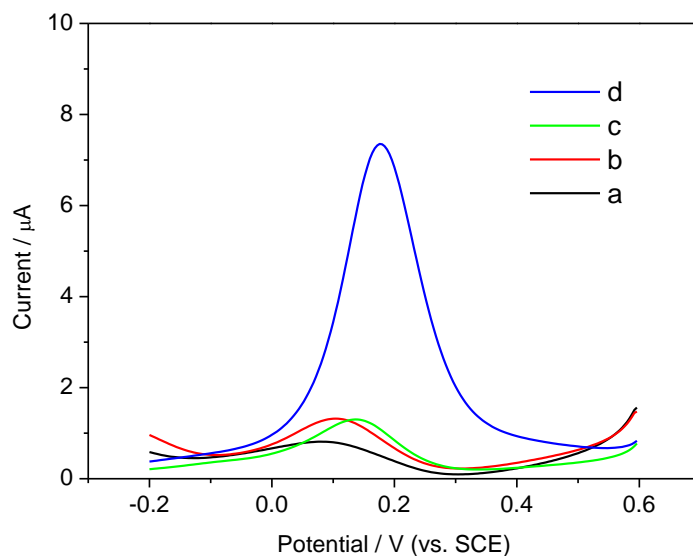


**Fig. S10** DPV curves of the HRP-imprinted SAM coated electrode from MDTG and PMBA/PATP before (a) and after (b) washing with aqueous acidic solution (pH = 3.1) and water and the HRP-imprinted SAM coated electrode from DHAP and PMBA/PATP before (c) and after (d) washing with aqueous acidic solution (pH = 3.1) and water. The DPV curves were measured in 10 mM PBS solution (pH = 7.4) of 2.5 mM  $\text{Fe}(\text{CN})_6^{4-/3-}$  and 0.1 M KCl.

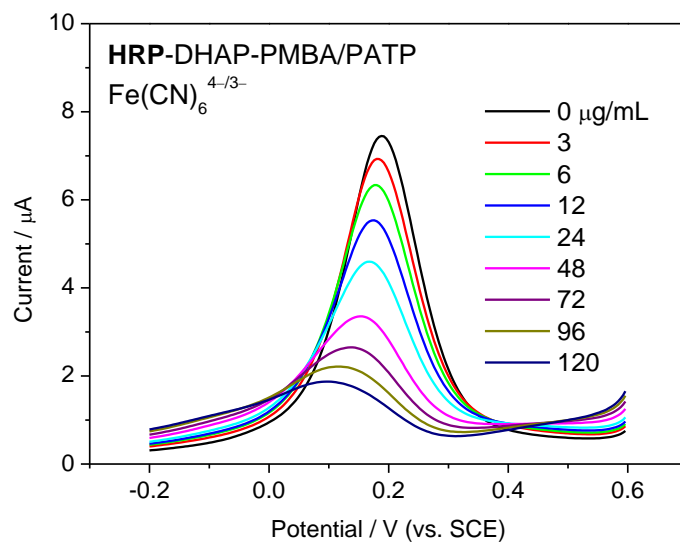


**Fig. S11** DPV curves of the HRP-imprinted coated electrode from DHAP and PMBA/PATP upon addition of HRP at different concentrations in 10 mM PBS solution (pH = 7.4) of 2.5 mM  $\text{Fe}(\text{CN})_6^{4-/3-}$  and 0.1 M KCl.

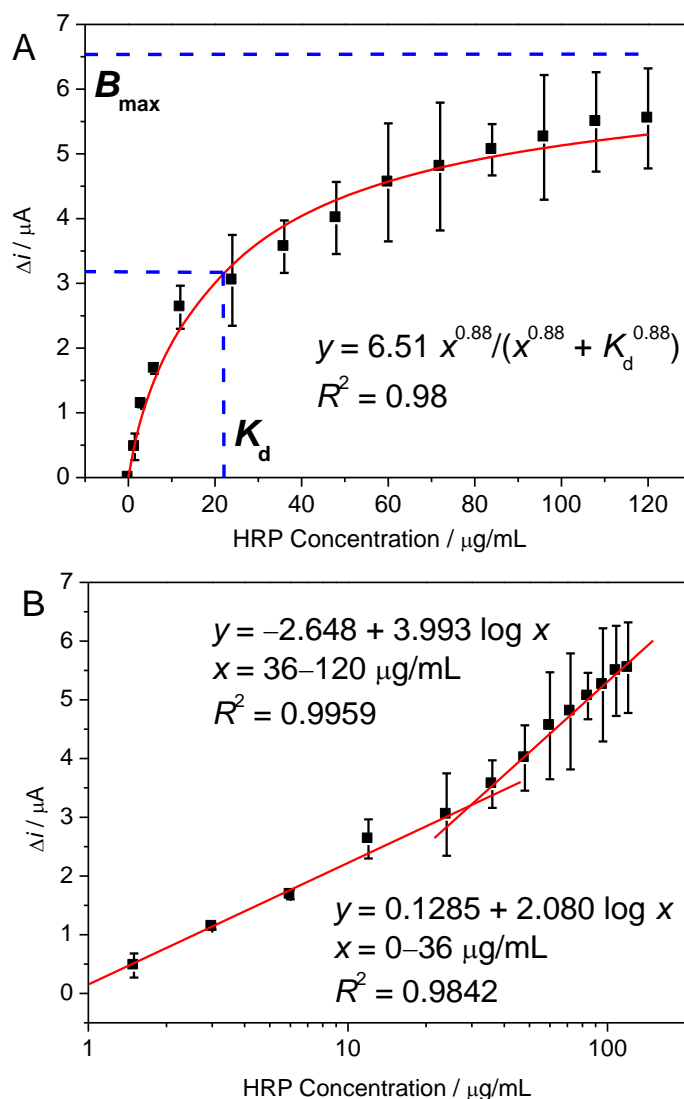


**Fig. S12** (A) Fitting of the HRP-imprinted coated electrode from DHAP and PMBA/PATP toward HRP of different concentrations using the Hill equation. (B) Bilinear plots of DPV current response of the HRP-imprinted electrode from DHAP and PMBA/PATP against logarithm of HRP concentration.

According to the Hill equation (eq S1),<sup>S2</sup>

$$y = B_{\max} x^n / (x^n + K_d^n) \quad (\text{S1})$$

where  $B_{\max}$  is the maximum specific binding,  $K_d$  is the dissociation constant, and  $n$  is Hill coefficient, the fitted  $K_d$  value was  $5.6 \times 10^{-7}$  M or 22.4  $\mu\text{g/mL}$  ( $R^2 = 0.98$ ,  $B_{\max} = 6.51$ , and  $n = 0.88$ ). The limit of detection of HRP was 1.18  $\mu\text{g/mL}$  ( $2.95 \times 10^{-8}$  M) at  $S/N = 3$ . Then, the complex stability constant ( $K_a$ ) of the imprinted SAM for HRP was obtained to be  $1.78 \times 10^6$   $\text{M}^{-1}$  (44.6 mL/ng).



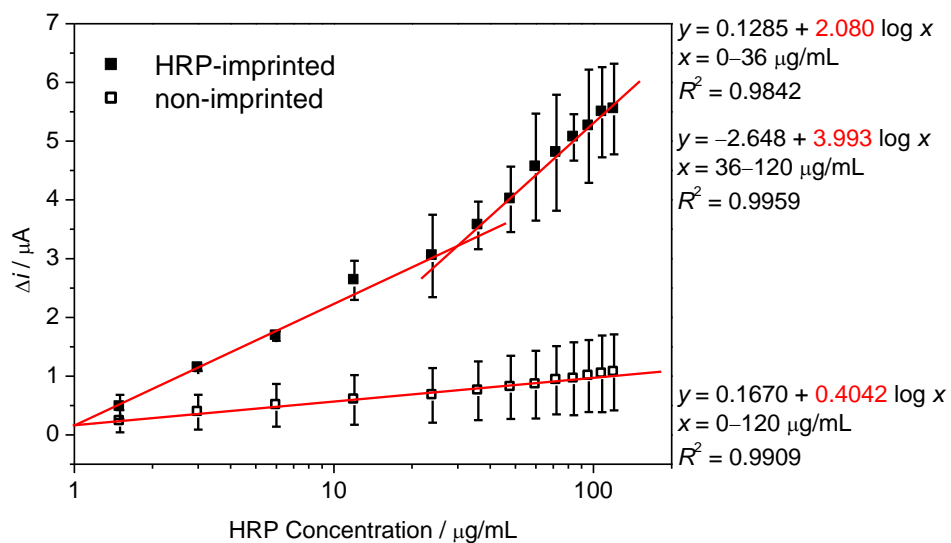


**Fig. S13** Bilinear plots of DPV current response of the HRP-imprinted SAM coated electrode from DHAP and PMBA/PATP and linear calibration plot of the non-imprinted counterpart against logarithm of HRP concentration.

The imprinting factor (IF) is defined as the ratio of the slope of the calibration plot for the imprinted SAM to that for the non-imprinted SAM. The IF of the HRP-imprinted SAM relative to the non-imprinted one was calculated to be 5.1 taking into account their calibration plots in the concentration range of 0–36  $\mu\text{g/mL}$ .

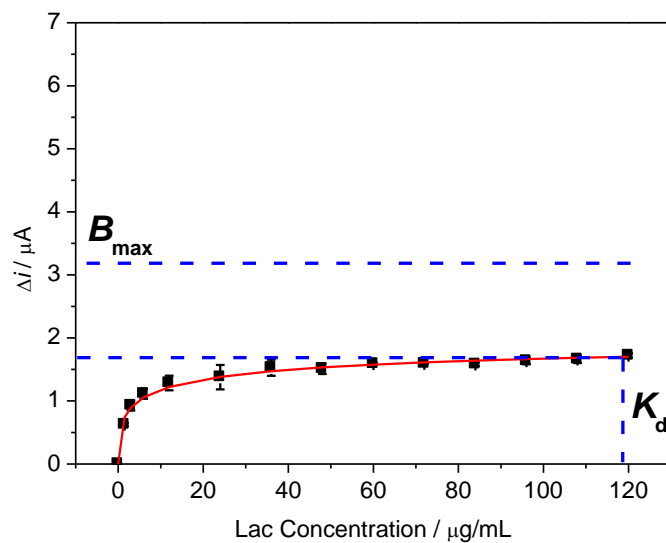


**Fig. S14** Fitting of the HRP-imprinted SAM coated electrode from DHAP and PMBA/PATP toward Lac of different concentrations using the Hill equation.

According to the Hill equation,<sup>S2</sup> the fitted  $K_d$  value was  $1.48 \times 10^{-6}$  M or 118  $\mu\text{g/mL}$  ( $R^2 = 0.95$ ,  $B_{\text{max}} = 3.2$ , and  $n = 0.233$ ). Then, the complex stability constant ( $K_a$ ) of the HRP-imprinted SAM for Lac was obtained to be  $6.76 \times 10^5 \text{ M}^{-1}$  (8.47 mL/ng).

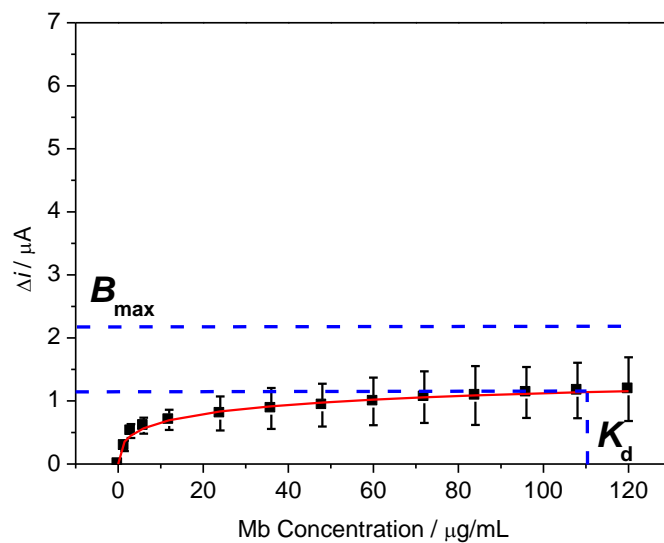


**Fig. S15** Fitting of the HRP-imprinted SAM coated electrode from DHAP and PMBA/PATP toward Mb of different concentrations using the Hill equation.

According to the Hill equation,<sup>S2</sup> the fitted  $K_d$  value was  $6.2 \times 10^{-6}$  M or 110  $\mu\text{g/mL}$  ( $R^2 = 0.98$ ,  $B_{\text{max}} = 2.2$ , and  $n = 0.358$ ). Then, the complex stability constant ( $K_a$ ) of the HRP-imprinted SAM for Mb was obtained to be  $1.61 \times 10^5 \text{ M}^{-1}$  (9.09 mL/ng).

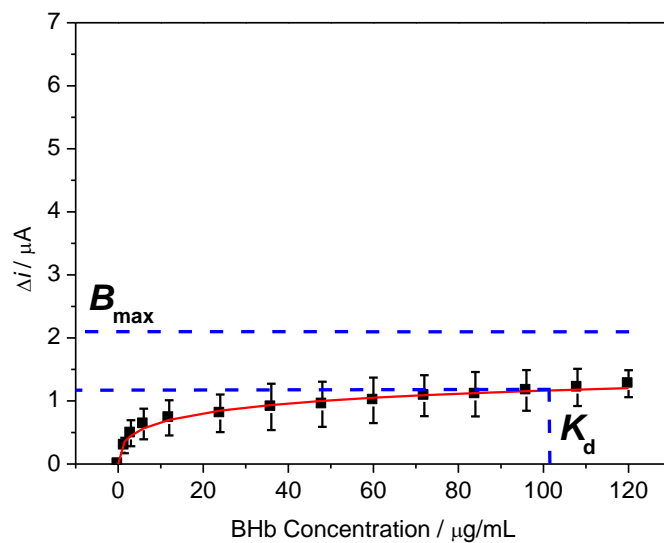


**Fig. S16** Fitting of the HRP-imprinted SAM coated electrode from DHAP and PMBA/PATP toward BHb of different concentrations using the Hill equation.

According to the Hill equation,<sup>S2</sup> the fitted  $K_d$  value was  $1.6 \times 10^{-6}$  M or 102  $\mu\text{g/mL}$  ( $R^2 = 0.95$ ,  $B_{\text{max}} = 2.1$ , and  $n = 0.308$ ). Then, the complex stability constant ( $K_a$ ) of the HRP-imprinted SAM for BHb was obtained to be  $6.25 \times 10^5 \text{ M}^{-1}$  (9.80 mL/ng).

**Table S2** Repeatability of HRP-imprinted coated electrodes at different batches after HRP extraction and upon rebinding of HRP at different concentrations.

electrode	DPV peak current ( <i>i</i> ) or change ( $\Delta i$ ) ( $\mu\text{A}$ )			mean value ( $\mu\text{A}$ )	standard deviation	relative standard deviation (%)
	electrode 1	electrode 2	electrode 3			
imprinted electrode after HRP removal	$i = 7.268$	$i = 7.556$	$i = 8.080$	7.635	0.4117	5.4
imprinted electrode upon rebinding of HRP (6 $\mu\text{g/mL}$ )	$\Delta i = 1.740$	$\Delta i = 1.625$	$\Delta i = 1.680$	1.682	0.0814	4.8
imprinted electrode upon rebinding of HRP (120 $\mu\text{g/mL}$ )	$\Delta i = 6.093$	$\Delta i = 5.001$	$\Delta i = 5.547$	5.547	0.7716	13.9

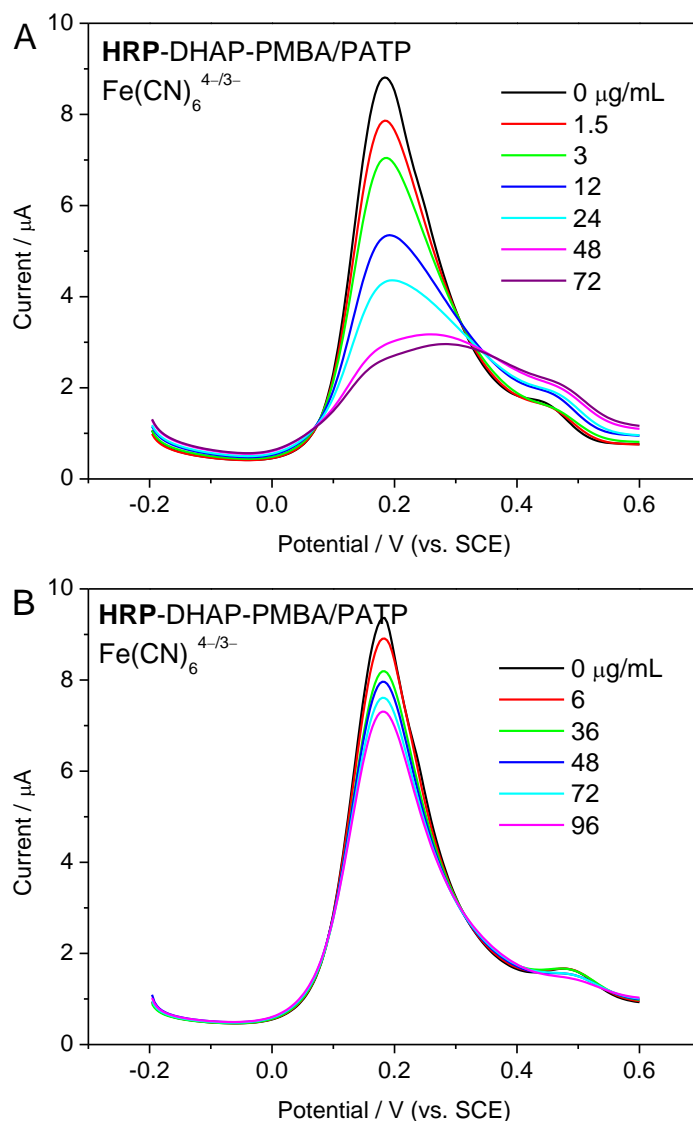


**Fig. S17** DPV curves of the HRP-imprinted coated electrodes from DHAP and PMBA/PATP upon addition of the mixed proteins of (A) HRP, Lac, Mb, and BHb (1:1:1:1 in weight) and (B) Lac, Mb, and BHb (1:1:1 in weight) with different concentrations of each protein in 10 mM PBS solution (pH = 7.4) of 2.5 mM  $\text{Fe}(\text{CN})_6^{4-/3-}$  and 0.1 M KCl.

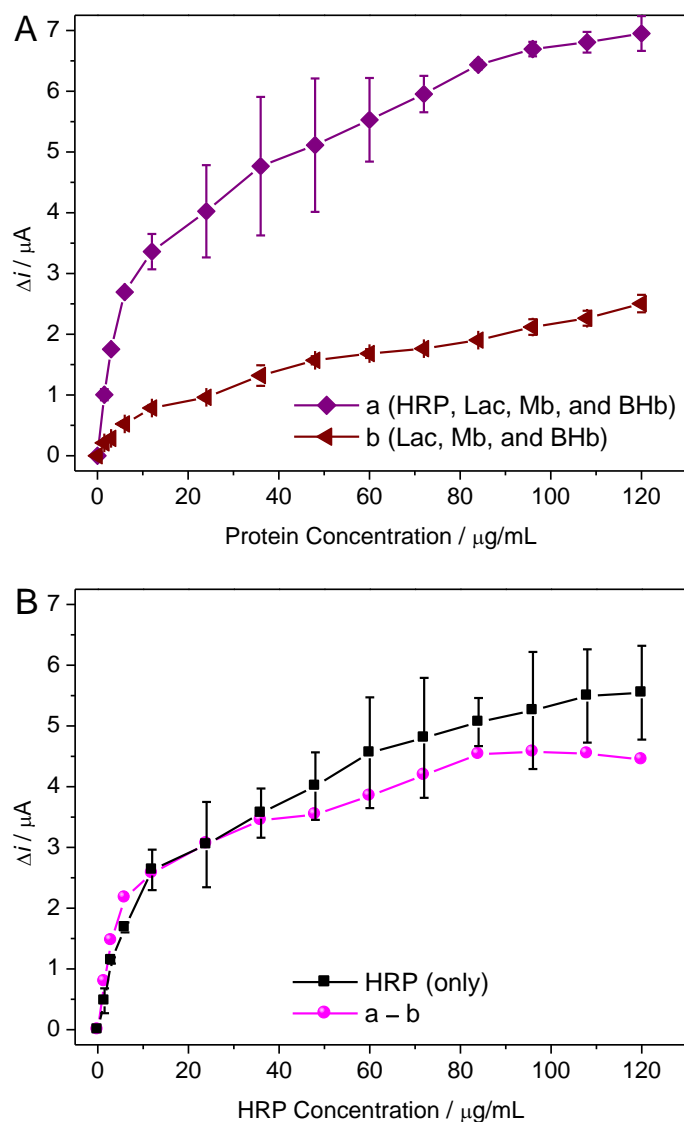


**Fig. S18** (A) Decrease of DPV cathodic peak current of the HRP-imprinted coated electrodes from DHAP and PMBA/PATP as a function of concentration of each protein of the mixed proteins of (a) HRP, Lac, Mb, and BHb (1:1:1:1 in weight) and (b) Lac, Mb, and BHb (1:1:1 in weight) and (B) Comparison of the difference between (a) and (b) with the decrease of DPV cathodic peak current of the HRP-imprinted coated electrode from DHAP and PMBA/PATP as a function of concentration of HRP only shown in **Fig. 4A** in 10 mM PBS solution (pH = 7.4) of 2.5 mM  $\text{Fe}(\text{CN})_6^{4-/3-}$  and 0.1 M KCl.

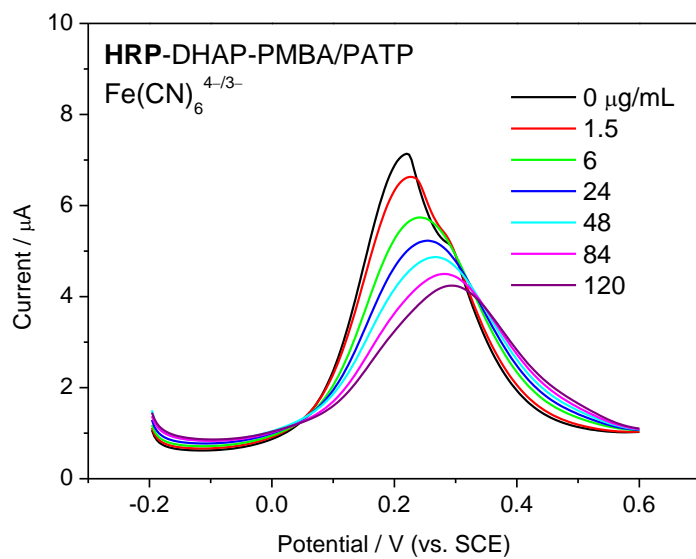


**Fig. S19** DPV curves of the HRP-imprinted coated electrode from DHAP and PMBA/PATP as a function of concentration of HRP in the presence of 1.17 mg/mL (6.5 mM) glucose in 10 mM PBS solution (pH = 7.4) of 2.5 mM Fe(CN)<sub>6</sub><sup>4-/3-</sup> and 0.1 M KCl.



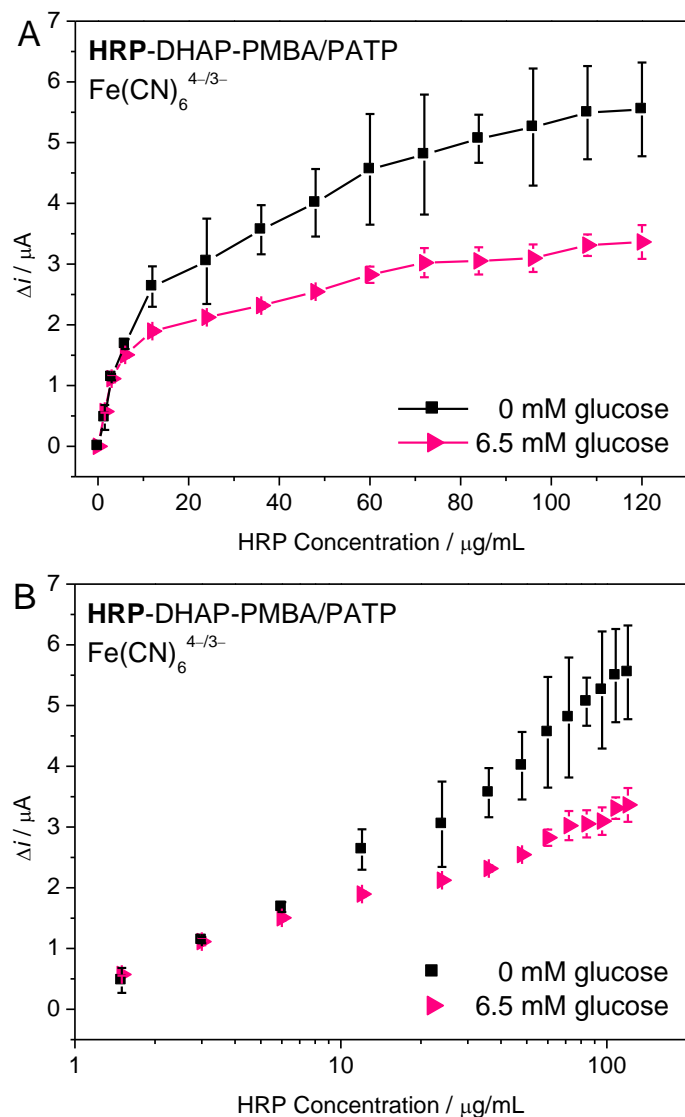


**Fig. S20** Decrease of DPV cathodic peak current of the HRP-imprinted coated electrode from DHAP and PMBA/PATP as a function of concentration of HRP in the presence of 1.17 mg/mL (6.5 mM) glucose in 10 mM PBS solution (pH = 7.4) of 2.5 mM  $\text{Fe}(\text{CN})_6^{4-/3-}$  and 0.1 M KCl: (A) linear scale; (B) logarithmic scale.

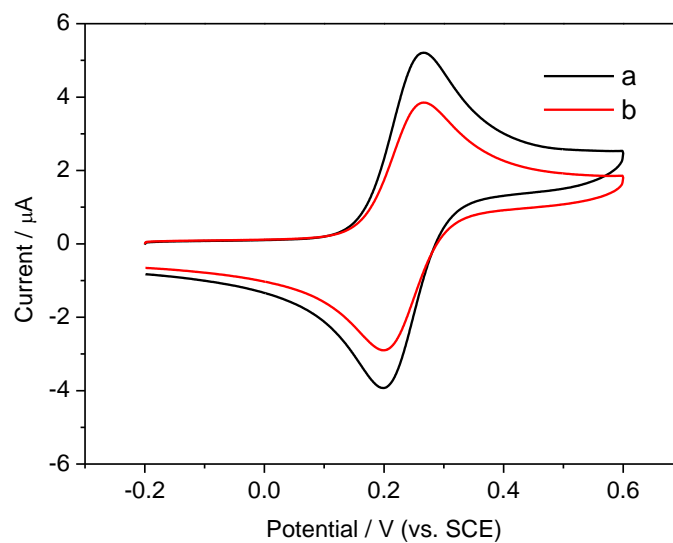


**Fig. S21** CV curves of the HRP-imprinted SAM coated electrode from DHAP and PMBA/PATP (a) after washing with aqueous acidic solution (pH = 3.1) and water and (b) upon addition of HRP (60  $\mu\text{g}/\text{mL}$ ) in 10 mM PBS solution (pH = 7.4) of 2.5 mM FcDM and 0.1 M KCl.

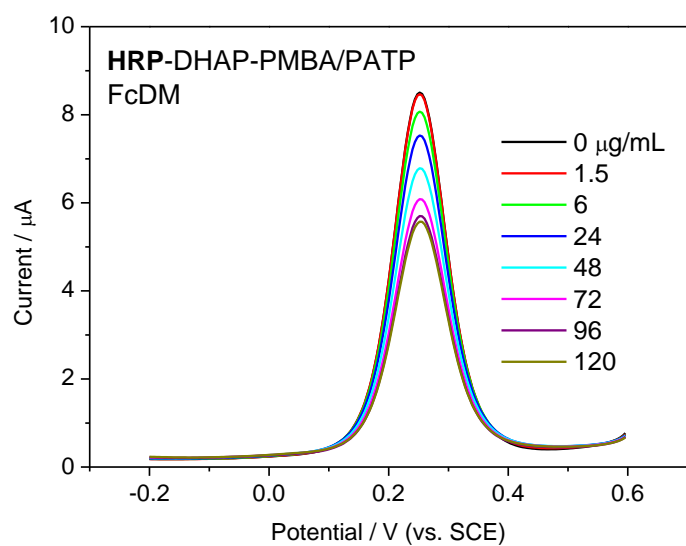


**Fig. S22** DPV cathodic peak currents of the HRP-imprinted SAM coated electrode from DHAP and PMBA/PATP upon addition of HRP of different concentrations in 10 mM PBS solution (pH = 7.4) of 2.5 mM FcDM and 0.1 M KCl.

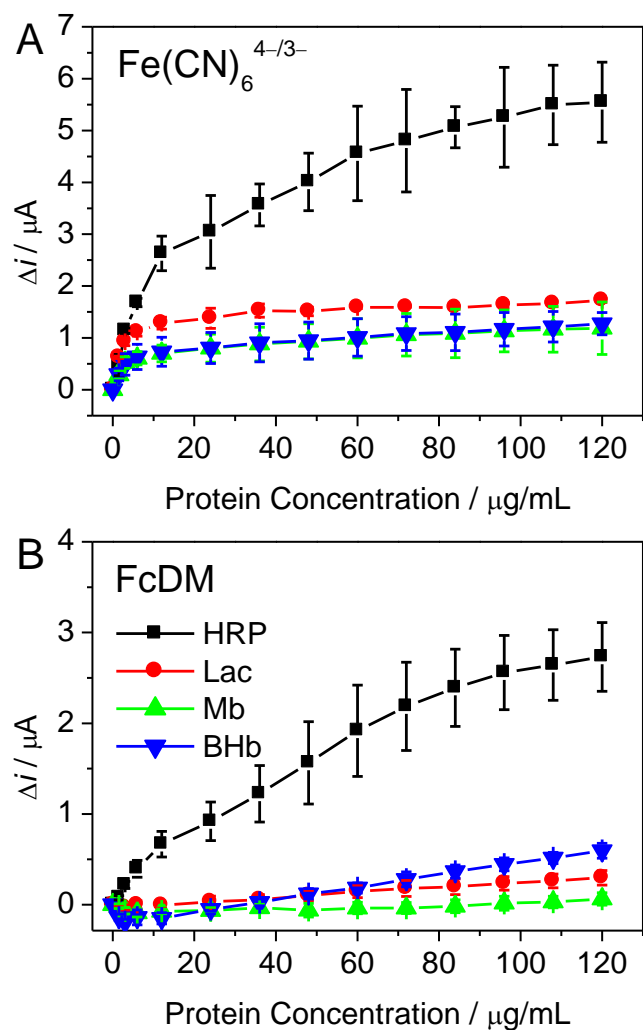


**Fig. S23** Decrease of DPV cathodic peak current of the HRP-imprinted SAM coated electrodes from DHAP and PMBA/PATP as a function of concentration of different proteins in 10 mM PBS solution (pH = 7.4) of 0.1 M KCl with different electroactive probes at 2.5 mM: (A)  $\text{Fe(CN)}_6^{4-/3-}$ ; (B) FcDM.

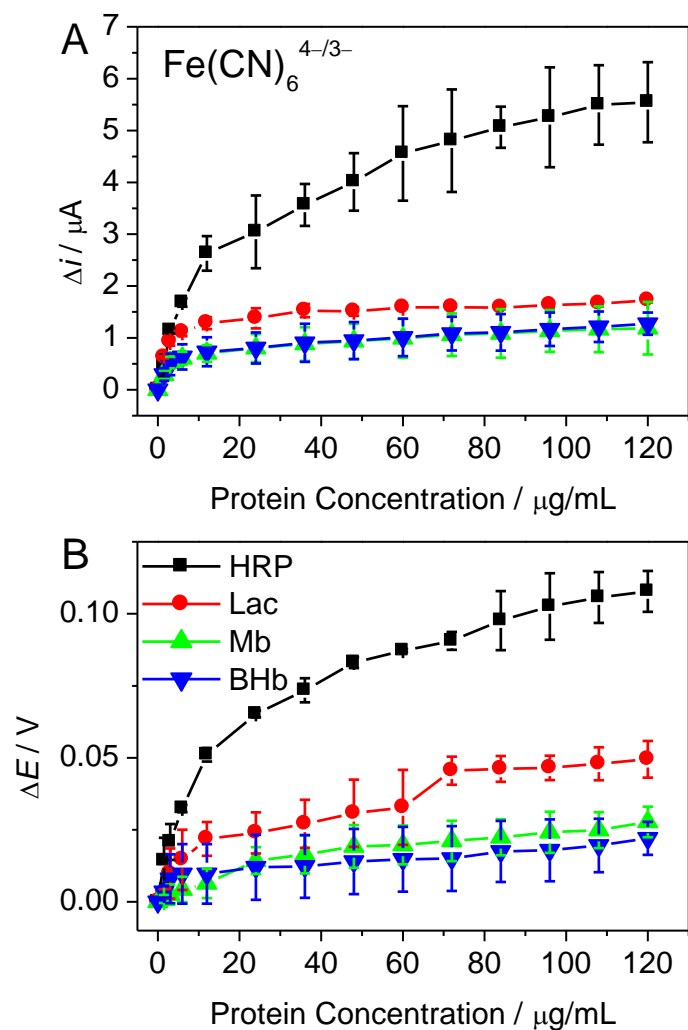


**Fig. S24** (A) Decrease of DPV cathodic peak current of the HRP-imprinted SAM coated electrodes from DHAP and PMBA/PATP as a function of concentration of different proteins in 10 mM PBS solution (pH = 7.4) of 2.5 mM  $\text{Fe}(\text{CN})_6^{4-/3-}$  and 0.1 M KCl. (B) Change of the open-circuit potential of the HRP-imprinted SAM coated electrodes from DHAP and PMBA/PATP as a function of concentration of different proteins in 10 mM PBS solution (pH = 7.4) of 0.1 M KCl.

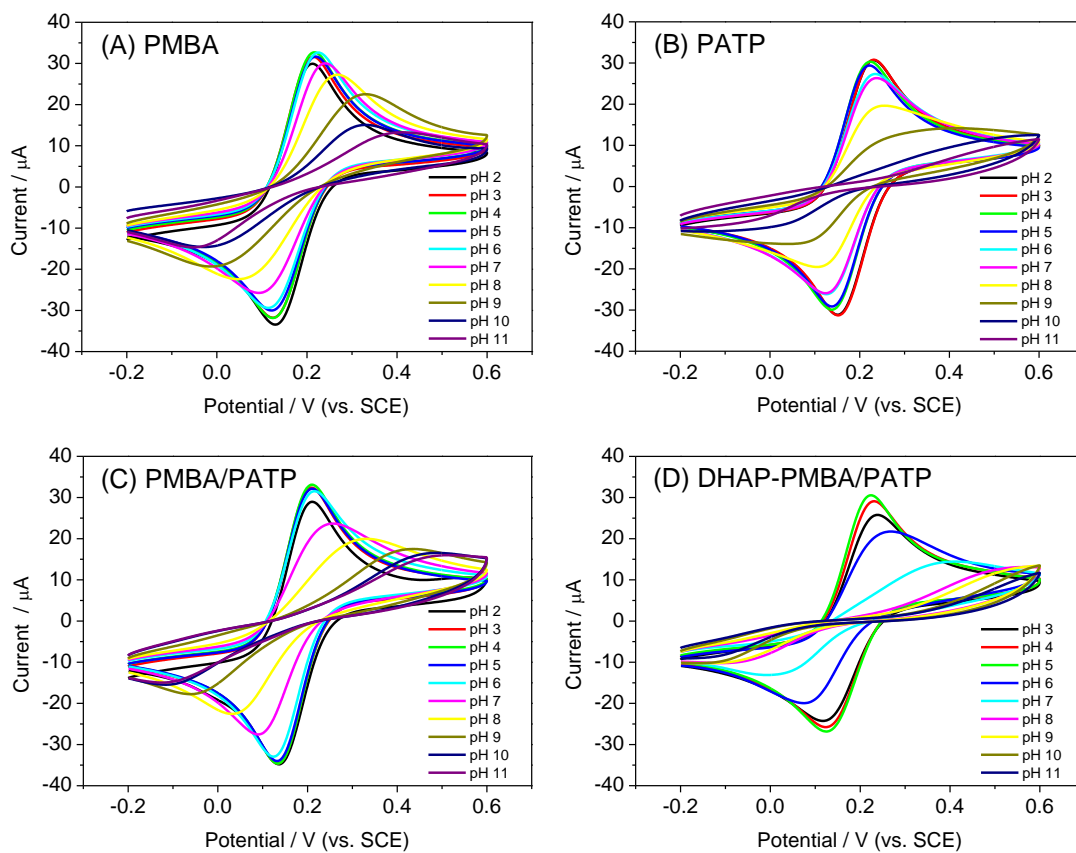


**Fig. S25** CV curves of the (A) PMBA-modified electrode, (B) PATP-modified electrode, (C) modified electrode from the equimolar mixture of PMBA and PATP, and (D) imprinted SAM coated electrode from DHAP and PMBA/PATP after HRP extraction as a function of pH in 10 mM PBS solution of 2.5 mM  $\text{Fe}(\text{CN})_6^{4-/3-}$  and 0.1 M KCl.

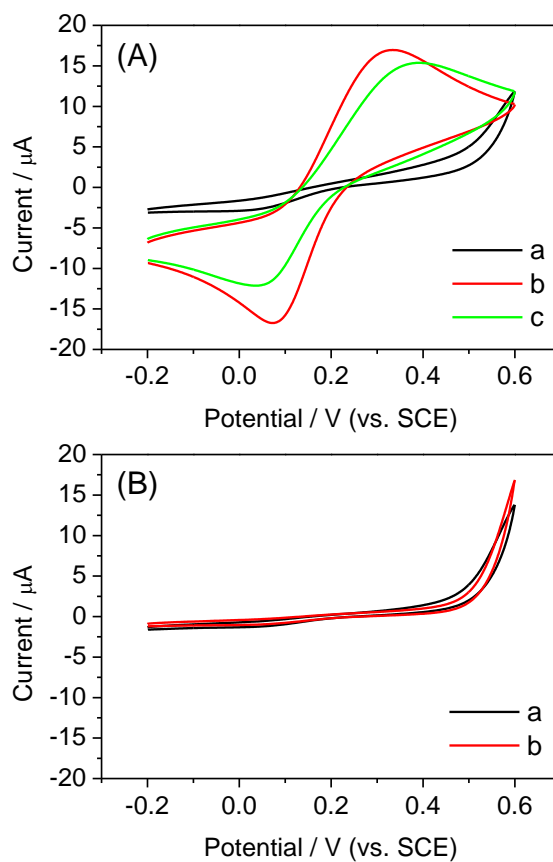


**Fig. S26** (A) CV curves of the Lac-imprinted SAM coated electrode from DHAP and PMBA/PATP (a) before and (b) after washing with aqueous acidic solution and water and (c) upon addition of Lac (36  $\mu\text{g/mL}$ ). (B) CV curves of the non-imprinted electrode from DHAP and PMBA/PATP (a) before and (b) after addition of Lac (36  $\mu\text{g/mL}$ ). The electrolyte solution used was 10 mM PBS solution ( $\text{pH} = 7.4$ ) of 2.5 mM  $\text{Fe}(\text{CN})_6^{4-/3-}$  and 0.1 M KCl.

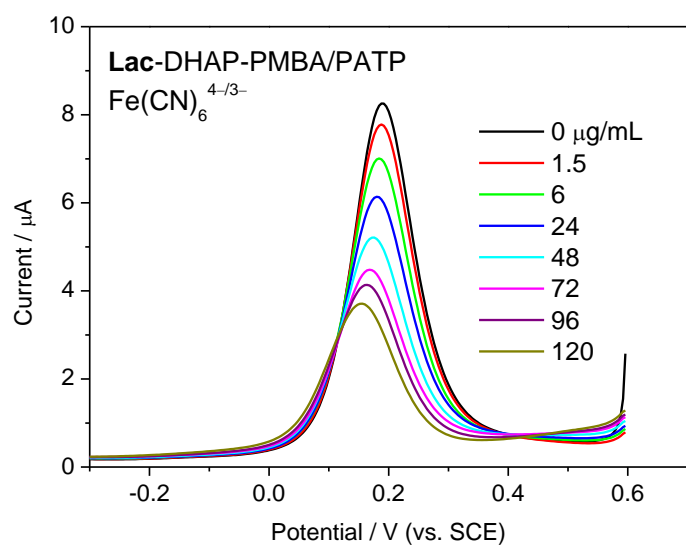


**Fig. S27** DPV cathodic peak currents of the Lac-imprinted SAM coated electrode from DHAP and PMBA/PATP upon addition of Lac of different concentrations in 10 mM PBS solution (pH = 7.4) of 2.5 mM  $\text{Fe}(\text{CN})_6^{4-/3-}$  and 0.1 M KCl.



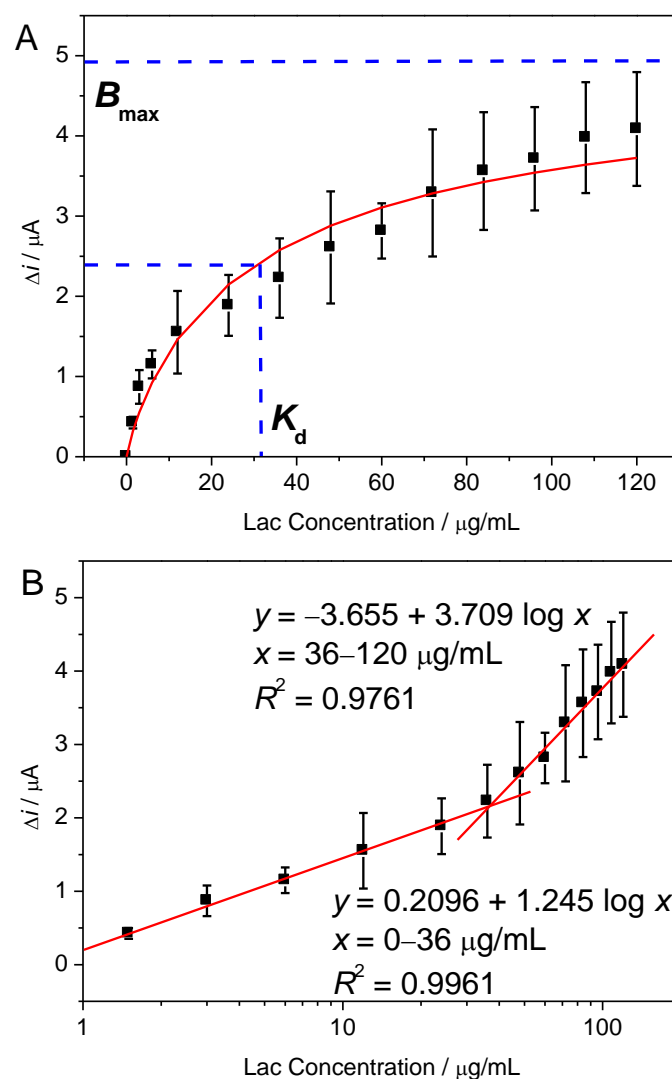


**Fig. S28** (A) Fitting of the Lac-imprinted SAM coated electrode from DHAP and PMBA/PATP toward Lac of different concentrations using the Hill equation. (B) Bilinear plots of DPV current response of the Lac-imprinted electrode from DHAP and PMBA/PATP against logarithm of Lac concentration.

According to the Hill equation,<sup>S2</sup> the fitted  $K_d$  value was  $4.0 \times 10^{-7}$  M or 31.9  $\mu\text{g/mL}$  ( $R^2 = 0.96$ ,  $B_{\text{max}} = 4.90$ , and  $n = 0.87$ ). The limit of detection of Lac was 1.43  $\mu\text{g/mL}$  ( $1.79 \times 10^{-8}$  M) at  $S/N = 3$ . Then, the complex stability constant ( $K_a$ ) of the imprinted SAM for Lac was obtained to be  $2.50 \times 10^6 \text{ M}^{-1}$  (31.3 mL/ng).

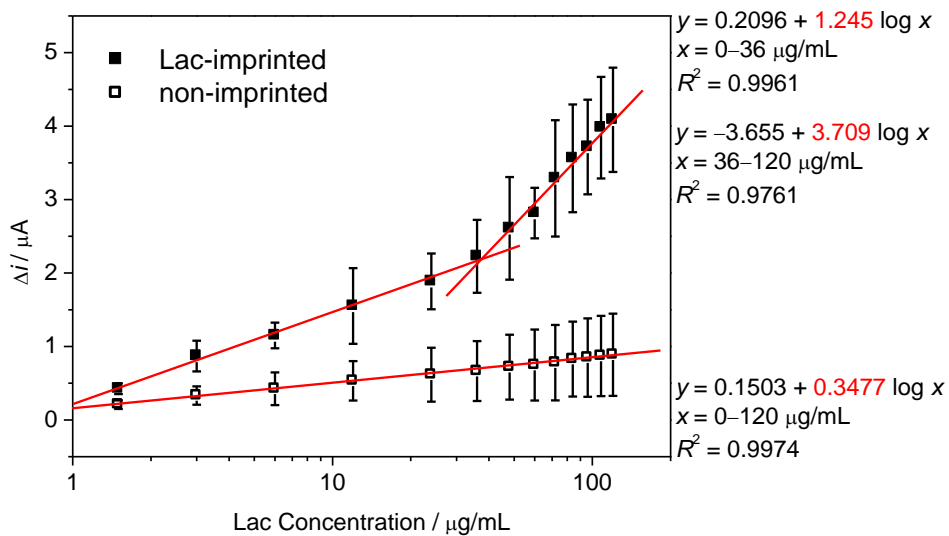


**Fig. S29** Bilinear plots of DPV current response of the Lac-imprinted SAM coated electrode from DHAP and PMBA/PATP and linear calibration plot of the non-imprinted counterpart against logarithm of Lac concentration.

The IF of the Lac-imprinted SAM relative to the non-imprinted one was calculated to be 3.6 taking into account their calibration plots in the concentration range of 0–36  $\mu\text{g/mL}$ .

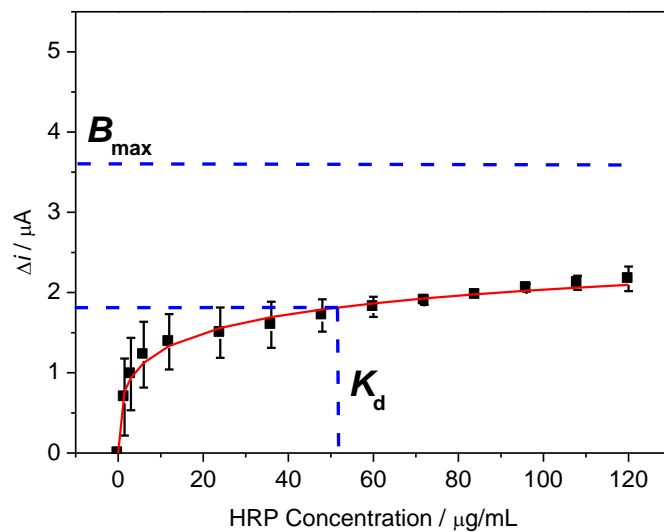


**Fig. S30** Fitting of the Lac-imprinted SAM coated electrode from DHAP and PMBA/PATP toward HRP of different concentrations using the Hill equation.

According to the Hill equation,<sup>S2</sup> the fitted  $K_d$  value was  $1.25 \times 10^{-6}$  M or 50.1  $\mu\text{g/mL}$  ( $R^2 = 0.99$ ,  $B_{\text{max}} = 3.61$ , and  $n = 0.373$ ). Then, the complex stability constant ( $K_a$ ) of the Lac-imprinted SAM for HRP was obtained to be  $8.00 \times 10^5$   $\text{M}^{-1}$  (20.0 mL/ng).

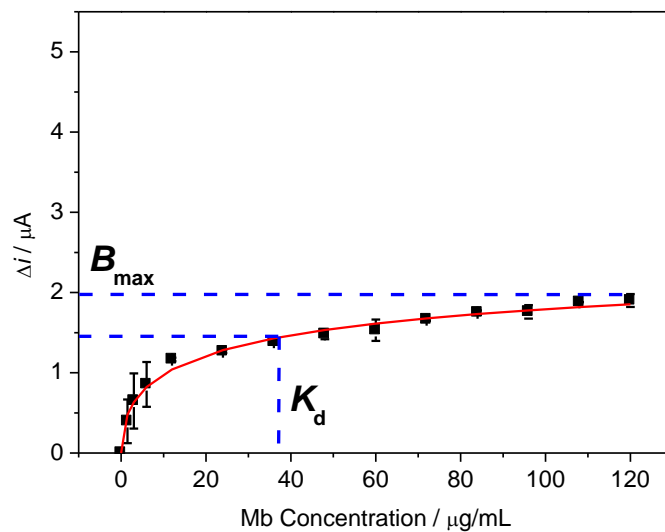


**Fig. S31** Fitting of the Lac-imprinted SAM coated electrode from DHAP and PMBA/PATP toward Mb of different concentrations using the Hill equation.

According to the Hill equation,<sup>S2</sup> the fitted  $K_d$  value was  $1.04 \times 10^{-6}$  M or 67.1  $\mu\text{g/mL}$  ( $R^2 = 0.99$ ,  $B_{\text{max}} = 1.99$ , and  $n = 0.448$ ). Then, the complex stability constant ( $K_a$ ) of the Lac-imprinted SAM for Mb was obtained to be  $9.61 \times 10^5$   $\text{M}^{-1}$  (14.9 mL/ng).

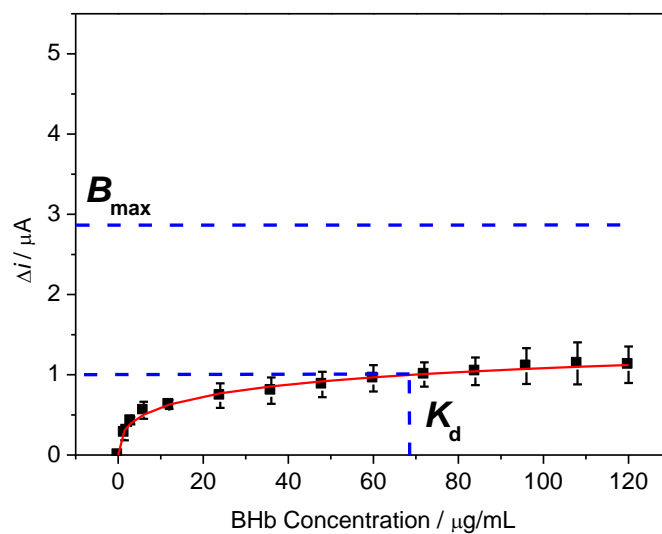


**Fig. S32** Fitting of the Lac-imprinted SAM coated electrode from DHAP and PMBA/PATP toward BHb of different concentrations using the Hill equation.

According to the Hill equation,<sup>S2</sup> the fitted  $K_d$  value was  $2.08 \times 10^{-6}$  M or 37.1  $\mu\text{g/mL}$  ( $R^2 = 0.99$ ,  $B_{\text{max}} = 2.88$ , and  $n = 0.503$ ). Then, the complex stability constant ( $K_a$ ) of the Lac-imprinted SAM for BHb was obtained to be  $4.81 \times 10^5$   $\text{M}^{-1}$  (26.9 mL/ng).

### Estimation of number density of imprinted cavities

If the imprinted cavities are assumed to act as independent disk-shaped nanoelectrodes and have average radii of template proteins estimated from their dimensions, approximate number density of imprinted cavities can be calculated using eq S2,<sup>S3</sup>

$$N = \frac{j}{4nFDC^*r_0} \quad (\text{S2})$$

where  $N$  is the number density of imprinted cavities,  $j$  is the current density and is obtained from CV data,  $r_0$  is the surface defect radius and is obtained from average radius of protein templates,  $F$  is the Faraday constant,  $D$  ( $D = 8.3 \times 10^{-6} \text{ cm}^2/\text{s}$  for  $\text{Fe}(\text{CN})_6^{4-/3-}$ ;<sup>S4</sup>  $D = 7.0 \times 10^{-6} \text{ cm}^2/\text{s}$  for  $\text{FcDM}^{\text{S5}}$ ) and  $C^*$  are the diffusion coefficient and bulk concentration of electroactive probes, respectively, and  $n$  is the number of electrons transferred per probe.

The application of eq S2 for determination of the number density of cavities imprinted in the SAM ( $N$ ) assumes that the diffusion coefficients of the redox probes in the aqueous solution and in the imprinted SAM were the same. However, typically, the latter is much lower. Therefore, it is clearly pointed out that the determined  $N$  value is at least the lowest possible limit of  $N$ .

### Estimation of fractional surface coverage of imprinted cavities

According to the theoretical model developed by Amatore et al.,<sup>S6</sup> the surface coverage of imprinted cavities is calculated approximately. The model is suitable for the chemical systems if diffusion is radial and the diffusion layers of the individual ultra-microelectrodes do not overlap. Fractional surface coverage of imprinted cavities,  $\theta$ , can be approximately calculated using eq S3,<sup>S6,S7</sup>

$$i_{\text{lim}} = nFSC^*D\theta/(0.6r_0) \quad (\text{S3})$$

where  $i_{\text{lim}}$  is the maximum limiting current and is obtained from CV data,  $n$  is the number of electrons transferred per electroactive probe,  $F$  is the Faraday constant,  $S$  is the geometrically projected surface area of the Au electrode ( $S = 0.0314 \text{ cm}^2$ ),  $C^*$  and  $D$  are the bulk concentration and diffusion coefficient of electroactive probes, respectively, and  $r_0$  is the average radius of imprinted cavities.

**Table S3** Comparison of the preparation parameters and performance of glycoprotein imprinted sensors based on boronate affinity.

glycoprotein imprinted sensor	glycoprotein	pH	glycoprotein assembly	initiator	method	$K_a$ ( $M^{-1}$ )	linear range ( $\mu\text{g/mL}$ )	limit of detection ( $\mu\text{g/mL}$ )	selectivity	reference
imprinted SAM	HRP	7.4	coassembly	no	DPV	$1.78 \times 10^6$	0–120	1.18	good	this work
imprinted SAM	Lac	7.4	coassembly	no	DPV	$2.50 \times 10^6$	0–120	1.43	good	this work
SAM & fluorinated phenylboronic acid & surface imprinting	ovalbumin	7.4	pre-assembly	yes	SPR	$4.7 \times 10^6$	0–100	1.32	good	S8
SAM & phenylboronic acid & surface imprinting	PSA	8.5	pre-assembly	yes	SPR	$5.6 \times 10^5$	N/A	N/A	good	S9
SAM & phenylboronic acid & surface imprinting	RNase B	8.5	pre-assembly	yes	SPR	$3.2 \times 10^5$	N/A	N/A	good	S9
graphene & phenylboronic acid & surface imprinting	ovalbumin	8.5	pre-assembly	$\text{NH}_3 \cdot \text{H}_2\text{O}$ (pH = 9.3)	DPV	$1.78 \times 10^6$	$1.0 \times 10^{-7}$ –0.1	$2.0 \times 10^{-8}$	good	S10
microplate & phenylboronic acid & surface imprinting	HRP	8.5	pre-assembly	yes	ELISA	$8.3 \times 10^8$	0–0.1	N/A	good	S11

SAM: self-assembled monolayer

DPV: differential pulse voltammetry

SPR: surface plasmon resonance

PSA: prostate specific antigen

ELISA: enzyme-linked immunosorbent assay

N/A: not available

## References

- (S1) X. Zhang, X. Du, X. Huang and Z. Lv, *J. Am. Chem. Soc.*, 2013, **135**, 9248–9251.
- (S2) S. Goutelle, M. Maurin, F. Rougier, X. Barbaut, L. Bourguignon, M. Ducher and P. Maire, *Fundam. Clin. Pharmacol.*, 2008, **22**, 633–648.
- (S3) O. Chailapakul and R. M. Crooks, *Langmuir*, 1995, **11**, 1329–1340.
- (S4) T. Y. Saji and S. Aoyagui, *J. Electroanal. Chem.*, 1975, **61**, 147–153.
- (S5) J. Guo and S. Amemiya, *Anal. Chem.*, 2005, **77**, 2147–2156.
- (S6) C. Amatore, J.-M. Savéant and D. Tessier, *J. Electroanal. Chem.*, 1983, **147**, 39–51.
- (S7) O. Chailapakul and R. M. Crooks, *Langmuir*, 1993, **9**, 884–888.
- (S8) T. Saeki, H. Sunayama, Y. Kitayama and T. Takeuchi, *Langmuir*, 2019, **35**, 1320–1326.
- (S9) A. Stephenson-Brown, A. L. Acton, J. A. Preece, J. S. Fossey and P.M. Mendes, *Chem. Sci.*, 2015, **6**, 5114–5119.
- (S10) J. Huang, Y. Wu, J. Cong, J. Luo and X. Liu, *Sens. Actuators B*, 2018, **259**, 1–9.
- (S11) X. Bi and Z. Liu, *Anal. Chem.*, 2014, **86**, 959–966.